Accepted Manuscript

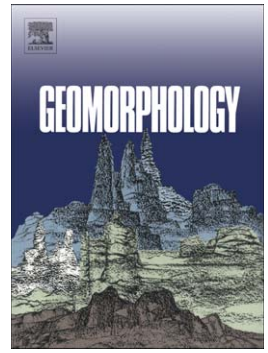

Analysis of landslide inventories for accurate prediction of debris-flow source areas

Jan Blahut, Cees J. van Westen, Simone Sterlacchini

PII: S0169-555X(10)00086-3
DOI: doi: 10.1016/j.geomorph.2010.02.017
Reference: GEOMOR 3209

To appear in: *Geomorphology*

Received date: 9 June 2009
Revised date: 18 February 2010
Accepted date: 23 February 2010

Please cite this article as: Blahut, Jan, van Westen, Cees J., Sterlacchini, Simone, Analysis of landslide inventories for accurate prediction of debris-flow source areas, *Geomorphology* (2010), doi: 10.1016/j.geomorph.2010.02.017

Analysis of landslide inventories for accurate prediction of debris-flow source areas

Jan Blahut [a,b,*], Cees J. van Westen [c], Simone Sterlacchini [b]

[a] Department of Environmental and Territorial Sciences, University of Milano-Bicocca, Piazza della Scienza 1, 20126 Milan, Italy

[b] Institute for the Dynamic of Environmental Processes, National Research Council (CNR-IDPA), Piazza della Scienza 1, 20126 Milan, Italy

[c] International Institute for Geo-Information Science and Earth Observation, ITC, Hengelosestraat 99 P.O. Box 6, 7500 AA, Enschede, The Netherlands

* Corresponding author. Tel.: +390 264 482 854, Fax: +390 264 482 895

E-mail address: jan.blahut@unimib.it (J. Blahut)

Abstract

For the generation of susceptibility maps on medium scales (1:25 000 to 1:50 000) using statistical techniques, a reliable landslide inventory is needed, together with factor maps used as inputs. This paper compares landslide susceptibility maps obtained with the same methodology but using different landslide inventories: the official Italian landslide inventory GeoIFFI for the Lombardy Region and a recently mapped inventory (DF2001). The analysis included four main steps: (i) preparation of debris flow inventories using both random and spatial partitions and factor maps as explanatory variables; (ii) calculation of accountability and reliability indices for a preliminary susceptibility analysis and selection of an appropriate combination of the factor maps for detailed analysis; (iii) evaluation and validation of the obtained susceptibility maps; and (iv) comparison of the results and selection of the final map. The study area is located in the Valtellina Valley in the Central Italian Alps. The analysis identified highly susceptible areas of shallow landslides that may generate debris flows. It was demonstrated that more

precisely delimited source areas for landslide-induced debris flows produce better susceptibility maps. However, the improvement of these maps was relatively limited when the inventories were randomly subdivided. Higher improvements were observed after the subdivision of the inventories into three geographical parts with different geomorphological characteristics. Although the modelling showed very similar results if evaluation is made using standard techniques, the spatial pattern of the susceptibility maps was highly variable and dependent on the combination of the factor maps used.

Keywords: Landslide inventory; Debris flow; Susceptibility analysis; GIS; Italian Alps

1. Introduction

Landslides are among the most significant natural damaging events in mountain environments. They are one of the primary causes of property damage, loss of life and injuries of persons. To better predict future occurrences of landslides and improve protection, hazard or susceptibility analyses are performed. Landslide susceptibility analysis (or so called spatial probability of landslide occurrence) using statistical techniques is based on the assessment of terrain conditions in an area subjected to previous landslides (Carrara et al., 1995). The conditions that caused the landslides are assumed to be the same for future landslides. Such a landslide susceptibility analysis on a medium scale (1:25 000 to 1:50 000) has been used as one of the first steps in landslide hazard assessment (Remondo et al., 2005; Fell et al., 2008). The performance of the models can be effectively evaluated and the prediction power of the models could be validated using techniques such as ROC curves to compute success and prediction rates based on areas under curves (Chung and Fabbri, 1999, 2003; Beguería, 2006).

A main problem in landslide hazard assessment is the definition of magnitude and frequency of prospective events. Although there are many methods for landslide susceptibility assessment, only a few techniques convert the result into landslide hazard maps based on temporal probability assessment. One of them is the use of event based inventory maps. The return periods of landslide triggering events are used for assessing temporal probability which is then combined with size and spatial probabilities generated from event-based inventories (Guzzetti et al., 2006a). However, only a few complete landslide inventories are available. Italy is one of the countries where such inventory databases have been made in a consistent manner.

This study focuses on the mapping of source areas of landslide-induced debris flows in the Valtellina Valley. According to Crosta et al. (1990), the majority of debris flows in the study area originate from soil-slips or shallow slides. They usually leave broad sheet-like scars which are easily recognizable on aerial photographs.

Statistically based susceptibility assessment for the source areas of landslide-induced debris flow was performed using different landslide inventories in order to evaluate the effect of the accuracy of the input data on the prediction capabilities of the resulting susceptibility maps. The same input data and analytical methods were used for all inventories. This study also evaluates the improvement of the predictions when the area is divided into geomorphologically homogeneous zones.

2. Study area

The study area, the Valtellina valley (Fig. 1), is a typical alpine valley located in the Lombardy Region in northern Italy. The valley has U-shaped transversal profiles derived from Quaternary glacial activity. The axis of the valley corresponds to the Adda River, flowing through the towns of Bormio, Tirano and

Sondrio to the Como Lake. The valley has prevalently an E□W orientation from Dubino to Teglio, where it enters the study area and takes an NE turn for a few kilometres, and then turns almost to N around after Grosio. The orientation of the valley is related to the location of a regional fault that separates the proper Alps (the Austroalpine, Penninic and Helvetic nappes) from the Variscan basement of the Southern Alps. This Periadriatic Fault (or so called Insubric Line or Tonale Fault) runs on the northern slopes of the valley, some 500 m above the Adda river floodplain. The bedrock in the valley is mainly composed of metamorphic rocks (gneiss, mica schist, phyllite and quartzite) and intrusive rock units, with subordinate sedimentary rocks. Due to the proximity of the fault, cataclastic and mylonitic zones are present. The alluvial plain of the Adda River is up to 3 km wide, and alluvial fans at the outlet of tributary valleys can reach a considerable size, with a longitudinal length up to 3 km.

Fig. 1 somewhere here

The study area lies in Consortium of Mountain Municipalities of Valtellina di Tirano, an area of about 450 km^2. Its territory is subdivided in 12 municipalities and has about 29,000 inhabitants, mainly on the valley bottom. The northern part of the study area is composed mainly of gneiss, while in the south micaschists and sedimentary rocks dominate. Both flanks of the valley are covered by morainic sediments and colluvial deposits of variable thickness. The bottom of the valley is covered by fluvial sediments. The lowest altitude in the study area is about 350 m a.s.l. near San Giacomo di Teglio where the Adda River flows out from the study area. The highest elevation is reached in the northern part of the study area on Cima Viola: 3370 m a.s.l.

The Valtellina Valley has a long history of intense and extensive landsliding. A large percentage of landslides are represented by rainfall-induced small slides and soil slips which are the sources for debris flows (up to 1.5 m thick), with volumes ranging from a few to thousands m^3 (Crosta et al., 1990, 2003). These phenomena affect cultivated areas, cause the interruption of transportation corridors and disrupt inhabited areas, sometimes leading to temporary evacuation of people. The study area suffered from intense rainfall and consequent landslides several times in the past. The major events occurred in 1983, 1987 and 2000.

In 1983 a severe precipitation event triggered more than 200 shallow landslides and debris flows between Tirano and Sondrio, with a density of 60 landslides per km^2 and causing 17 casualties (Cancelli and Nova, 1985). Two major storms were observed on May 14th to 16th and May 21st to 23rd, 1983, in the Valtellina valley. In Aprica a cumulated precipitation of 453 mm was measured which corresponds to 34% of the total annual precipitation. The average cumulative rainfall for the whole event was in the order of 260 mm (Guzzetti et al., 1992). The most affected part of the study area was in Tresenda (a part of Teglio Municipality) where a debris flow caused 14 casualties.

Another series of major event occurring in July 1987 claimed 12 lives and triggered several hundreds of soil slips and debris flows (Crosta, 1990; Crosta et al., 2003). The main rainfall event occurred on July 17th to 19th and was marked by increasing rainfall intensity (Guzzetti et al., 1992). Unfortunately a complete landslide inventory was not compiled, mainly because of the constraints of time and resources (Guzzetti et al., 1992). Aerial photographs after the 1987 event are limited to a narrow strip along the Adda River and do not allow us to map the source areas of the landslides.

Landslides affecting the Valtellina Valley on November 14th to 17th, 2000, were mostly concentrated on terraced slopes used as vineyards. A prolonged intense rainfall event triggered 260 shallow landslides on an area of 270 km^2. The highest landslide density was observed around Bianzone, with 49 landslides per

km^2, and near Tirano with 26.8 landslides km^{-2} (Crosta et al., 2003).

In order to capture different characteristics of debris flow source areas in the different places (Fig. 2) of the studied area, the landslide inventories were divided in three subsets: Northern, Central and Southern parts (Fig. 3). The Northern subset lies in the Val Grosina Valleys, which are two tributary valleys belonging to the Rhaetic Alps. They represent the highest altitudes in the area with typical alpine relief. Glaciers played a major role in the development of the morphology and they are still present in a limited area in the highest altitudes. The majority of this area is underlain by gneiss bedrock. Rock glaciers and landslide deposits are typical in this part of the territory. The central subset lies on both flanks of the Valtellina Valley. Slopes are covered mainly by moraine deposits. On both flanks Pleistocene glacial terraces are present. The Southern subset covers five parallel valleys among which Val Belviso is the largest one. The southern territory is mainly composed of micaschists but sedimentary rocks are also present in the southernmost part. Geomorphologically it is part of the Orobic Alps.

Fig. 2 somewhere here

Fig. 3 somewhere here

3. Materials and methods

In order to compare susceptibility maps created from different inventories, the methodology presented in Fig. 4 was applied. First, the existing landslide inventory was compared with a newly generated inventory. Based on an initial set of factor maps, the accountability and reliability indices were estimated to choose different combinations of factor maps as inputs for Weights-of-Evidence (WofE) modelling.

The two landslide inventories were randomly and spatially subdivided and WofE modelling was applied to create susceptibility models. The model performance and prediction power of the susceptibility maps was assessed using success and prediction rate curves with corresponding areas under curves (Chung and Fabbri, 1999, 2003). Afterwards, highly performing models were compared and their spatial variability was assessed. Finally, the best model was chosen to create the final debris flow susceptibility map.

Fig. 4 somewhere here

3.1. Landslide inventories

There are three official landslide inventory databases available for the study area:

- The AVI database: A bibliographical and archive inventory of landslides and floods in Italy (Guzzetti et al., 1994), which is updated regularly. The AVI Database was originally designed to inventorize all places in Italy which were affected by landslides or floods. No spatial scale was defined for this database, and the information was visualized as points with coordinates.
- The regional database of landslides of the Lombardy Region (Lombardy Region, 2002), mapped at 1:10,000 scale. This database has been compiled since 1998 and is systematically updated.
- The GeoIFFI landslide inventory database for the Lombardy Region (GeoIFFI, 2006), which is part of the IFFI National Database.

Unfortunately, there is only limited information about debris flow source areas in the AVI and Lombardy Regional databases. In the AVI database there are a total of 80 events within the study area, but only 12 of them are classified as debris flows and only three events have a precise date (day, month and year). In the Lombardy database there are 501 events within the study area, of which 46 are classified as debris flows, but only seven have information about the exact date of occurrence. Another problem with these databases is related to the spatial location of the events. Both databases have coordinates showing event locations but only in some cases the points are located in the scarp areas, and mostly they are in the transport or deposition areas.

The GeoIFFI database was made by incorporating the two previously mentioned inventories. The database consists of different types of landslides such as debris flows, earth flows, shallow landslides, and deep seated gravitational slope deformations mapped by points, lines, and polygons. Unfortunately, there is no information on the time of occurrence of the debris flows; thus, it is impossible to divide the inventory into temporal subsets. For this study, only debris flow scarp areas mapped as points were considered because there are only a few debris flows mapped as polygons or lines in the database. Moreover, in the case of polygons and lines, the scarp areas may not be clearly distinguishable from the rest of the flow.

The GEoIFFI inventory contained 1,478 landslide scarps. Because the inventory included mistakes with the positions of the scarps, we decided to make a new inventory (abbreviated as DF2001). We prepared this inventory by the interpretation of aerial photographs taken in 2001. A total of 573 landslide scarp polygons (with a total area of 4.4 km^2) were mapped. The ILWIS software (ITC, 2009) was used for the precise delimitation of the scarp polygons using the aerial photographs and a DEM. The DF2001 inventory has several advantages compared to the GeoIFFI database such as the use of polygons as mapping units instead of points of GeoIFFI database (Fig. 5) and the exclusion of the debris flow scarps that were initiated on anthropogenic terraced terrain due to the collapse of man-made dry stone walls supporting the terraces. Because of the scale of this study and a lack of data about the present state of these dry stone walls, only natural landslide-induced debris flow scarps were taken into account.

Fig. 5 somewhere here

Both the GeoIFFI and the DF2001 inventories were randomly subdivided into two subsets with the same size. As already mentioned, both inventories were also spatially subdivided into the three subsets. The training subsets were used for the construction of the model, and the validation subset was used for independent validation of the predictive power of the resulting models.

3.2. Factor maps

After evaluating the literature (Carrara et al., 1991; Soeters and van Westen, 1996; Guzzetti et al., 1999; Castellanos Abella, 2008), 10 causal factor maps were prepared (Fig. 6). These maps can be divided in two groups: DEM derived factors and other geo-factors.

Fig. 6 somewhere here

For the preparation of these maps, a DEM of the study area with a 10 m resolution was used. The DEM was provided by the Cartographical Office of the Mountain Consortium of Municipalities of Valtellina di Tirano, from contour lines with an interval of 1 m in urbanized areas and 10 m in the rest of the territory, and additional points with spot heights obtained by photogrammetry from the 2001 air photos. The following factors were derived from the DEM using ArcGIS tools: altitude, internal relief, planar curvature, profile curvature, slope, slope aspects, and flow accumulation. The values of each factor were classified into 10 classes using quantiles, except for the aspect map, which had nine classes (eight for the main compass directions and one for flat areas).

Usage of quantile classification may cause important consequences if data distribution is extremely skewed. The usage may make it possible to better explore the behaviour of the factors with respect to the landslide occurrence, because the rank-ordered variables are proportionally distributed.
For the preparation of the geo-factor maps several sources were used:

- A land use map, derived from the 1:10 000 scale map of DUSAF Project (2003), made by the Lombardy Region using orthophotos taken in 2001. The map contains 23 classes of which the largest ones are coniferous trees and scarce vegetation.
- A geological surface material map, rasterized from a 1:10 000 scale geological map of the Lombardy Region generated by CARG Project (1992). The map contains 51 classes of lithological as well as soil cover units mapped directly in the field and by air photo interpretation. Morainic deposits and gneiss rocks represent the most frequent classes.
- A distance to faults map, derived using tectonic lines extracted from the 1:10 000 tectonic map from CARG Project (1992). Local experts suggest that the effect of the major faults in the study area on landslide occurrence, due to the possible deterioration of the physical and mechanical characteristics of rock masses along tectonic lines and thus the higher availability of loose material, may extend up to 500 m from a fault. Thus a six class map was prepared with different buffer limits (25, 50, 100, 250 and 500 m).

3.3. Methodology

3.3.1. Basic weights estimation, accountability and reliability

As a first step in the susceptibility analysis, the prior probabilities were estimated as overall debris flow scarp densities. For the GeoIFFI database, the prior probability of landslide scarps was relatively small (0.000327) as scarps are represented by 1478 10×10 m cells) in an area of ca. 450 km^2 (4,515,418 cells). Using 573 polygons in the DF2001 database, rasterized as 43,846 10×10 m cells, the prior probability was estimated to be 0.00971. After the subdivision of the inventories in the random and spatial subsets, the prior probabilities obviously declined.

Subsequently the ten factor maps were overlaid with the two landslide inventories in order to calculate the densities of scarps in all classes of each factor map. These densities were then compared with the prior probabilities discussed above.

For the analysis of the different factors contributing to debris flow triggering, two estimators called "accountability" and "reliability" were employed. They were introduced by Greenbaum et al. (1995a,b) and used by Castellanos Abella (2008) as simple indicators of the importance of particular classes of factor maps. The accountability is calculated as the sum of landslide cells in those classes of factor maps with a landslide density greater than the average density in the whole area, divided by the sum of landslide cells over the whole area and multiplied by 100. The reliability is calculated as the sum of landslide cells in those classes of factor maps with density values greater than the average density in the whole area, divided by the area of these classes and multiplied by 100 (Castellanos Abella, 2008). The accountability index explains how the classes of factor maps that are relevant for the analysis (with densities higher than regional average) contain landslide cells. The reliability index gives an idea of the average landslide density in the classes of factor maps that are relevant for landslide occurrence (with values higher than 1). Both indicators provide different but relevant results for landslide prediction, although the reliability index is more important (Greenbaum et al., 1995a,b). Using these indicators it is possible to identify the relevance of each factor to landslide occurrence. Moreover, it is possible to better choose the appropriate combination of the most relevant factor classes for the model construction. The main drawback of using the accountability and reliability indices is that they cannot distinguish particular classes which are relevant within the factor maps. The accountability and reliability indices were calculated for both the GeoIFFI and DF2001 databases as well as for their spatial subsets.

3.3.2. Weights-of-Evidence

The Weights-of-Evidence modelling technique (WofE) was applied to analyse the debris flow susceptibility. Since the 1990s this method has been used for landslide susceptibility evaluation (van Westen, 1993; van Westen et al., 2003; Süzen and Doyuran, 2004, Thierry et al., 2007). The modelling technique applied is well known, so only a basic introduction is presented here. For further information about the method the reader is referred to Bonham-Carter et al. (1988) and Agterberg et al. (1989). WofE utilizes a combination of different spatial datasets (evidential themes or factor maps) in order to analyse and describe their interactions and generate predictive models (Bonham-Carter, 1994; Raines et al., 2000). WofE is a data-driven process that uses known occurrences (training points or response variables) as model training sites to produce predictive probability maps (response themes) from multiple weighted evidences (Raines, 1999). Training points are used in WofE to calculate prior probability, weights of each of the evidential thematic classes, and posterior probabilities of the response theme. The WofE model uses a log-linear form of the Bayesian probability function. The prior probability that an event occurs per unit area is calculated as the total number of events over the total area. This initial estimate can be later increased or diminished in different areas by the use of available explanatory variables. The method is based on the calculation of positive and negative weights by which the degree of spatial association among events, and explanatory variables may be modelled.

An ArcGIS 9.2 extension (SDM – Spatial Data Modeller; Sawatzky et al., 2008) was used for an automatic and iterative calculation of the models. As already mentioned in many studies (Thierry et al., 2007; Castellanos Abella, 2008), WofE has an assumption of conditional independence between variables that, if it is not verified, may lead to an overestimation of spatial probabilities. In natural conditions, many factor variables have some dependence (e.g., altitude and land use; faults and geology; and slope and internal relief). To overcome this problem, weight values of the resulting susceptibility map were treated as relative and not absolute values. Thus, the probability values were ordered from the highest to the lowest ones and, consequently, reclassified into classes. Moreover, as mentioned by Bonham-Carter (1996), WofE provides a simplification that, when used carefully, represents relative contributions of the separate factors. Therefore, it is often used as a selection procedure for multivariate statistical analysis.

3.3.3. Success rate curves

Success rate curves – SRCs (Chung and Fabbri, 1999) were used to assess the performances of the models. SRCs are made by plotting the cumulative percentage of susceptible areas (starting from the highest probability values to the lowest ones) on the X axis and the cumulative percentage of corresponding training points on the Y axis. The steeper the curve the better the capability of the model is to describe the distribution of landslides. The steepness of the curve also depends on the landslide distribution in the area. In a situation when a large portion of the area is covered by landslides, it is impossible to get steep curves.

3.3.4. Prediction rate curves

The last step of the analysis was aimed at evaluating the predictive power of the maps using prediction rate curves – PRCs (Chung and Fabbri, 2003). PRCs are made in the same way as SRCs; but instead of the training subset, a prediction subset (of the scarps that were not used as training subset) is used. For the randomly divided inventories the second subset which did not enter into the model calculation was used to calculate correspondent prediction rate curves. The predictive power of the three spatially divided inventory subsets was analysed by cross-validation (e.g. using the central and southern subsets for quantifying the predictive power of the northern subset). The intention of this cross-validation technique was to examine different causal factors of debris flows in different parts of the study area. Moreover, the prediction power of the models, developed using subsets from other parts of the study region, was also analysed. Nevertheless, to evaluate the real predictive capabilities of the model, a multi-temporal landslide inventory should be used, because some of the factors, like land use, might have changed in the period between the two landslide inventories of different periods. The model should be made using an older landslide inventory, and more recent landslides should be used for the evaluation of the prediction, as applied by Guzzetti et al. (2006b) and Chung and Fabbri (2008).

To summarize SRCs and PRCs for models form the different inventories, the area under the curve (*AUC*) was calculated. This area is expressed as a percentage of the graph that lies under the curve and allows an easy comparison of SRCs and PRCs from different models. As already stated by Carrara et al. (2008), evaluation of the prediction power of the models is always a difficult task and all known approaches suffer from conceptual or operational pitfalls. This study mainly uses the PRC method for supporting the model results and assessing the robustness of the model.

4. Results and discussion

4.1. Landslide densities

The three highest and three lowest density values in the classes of the five most relevant factor maps are summarized in Table 1. Although there are no large differences among the highest and lowest density classes for the two inventories, the density values differ a lot because the DF2001 inventory has a much wider area extent than the GeoIFFI inventory. The highest densities are present in the largest classes of slope angle, internal relief and planar curvature and in land use classes of bare land and scarce vegetation. Although geology classes with the highest scarp densities are sandstones and claystones, they occupy only a very small portion in the southern part of the study area. The lowest scarp densities are observed in low slope, planar curvature and internal relief classes, and in pastures, mixed and broadleaf forests. Differences between the GeoIFFI and DF2001 inventories exist in the low landslide density classes of the geological map. GeoIFFI has low densities for paleolandslide and alluvial-colluvial deposits, while DF2001 has low densities for conglomerate and morainic sediments. However the lowest density class is represented by colonized scree slopes in both cases.

Table 1. somewhere here

4.2. Accountability and reliability

The accountability and reliability indices calculated for the factor maps are shown in Table 2. When assessing the whole area using the GeoIFFI database, the factor maps with the highest accountability and reliability values are altitude, land use, geology and slope. No association was found with profile curvature, aspect and fault distance. The accountability scores for the DF2001 database are consistently higher than those for the GeoIFFI database. This means that the DF2001 database has a better discriminating power of separating relevant classes for landslide occurrence. This can be probably caused by considering the whole scarp polygon in the DF2001 database, instead of the GeoIFFI database where scarps are mapped as single points. Thus, more information is kept in the new DF2001 database. The DF2001 database shows factors with high indices similar to those for the GeoIFFI database, and internal relief and planar curvature play a more important role. The reliability indices, which are indicators of the average landslide density in the classes that are important for the landslide triggering, are much higher for the DF2001 database. However, it is not methodologically correct to compare the indices between the GeoIFFI and DF2001 databases as the former is based on points (represented by 1478 10×10 m cells, with a total area of 0.15 km^2) and the latter on polygons with much larger total area (4.4 km^2). The reliability indices in both databases show the highest values in altitude, internal relief, land use, geology, planar curvature, and slope factor maps.

According to field surveys, substantial differences in the debris flow predisposing factors are expected in different portions of the study area. Therefore also separate analysis was done for the three sub-areas (Fig. 7). The differences in debris flow sources are mostly caused by particular geological characteristics in different parts of the area. In the northern part, gneiss outcrops have a much higher influence on debris flow initiation, than in the rest of the study area. In the southern part, debris flows initiate mostly on slopes underlain by sandstones and other sedimentary rocks. In the central part the most common rock type in debris flow source areas is micaschists. Also many debris flow source areas indicated in the DF2001 database are underlain by colluvial deposits.

Table 2 somewhere here

Fig. 7 somewhere here

Analysis of the northern subset shows that land use and geology together with slope, internal relief and altitude are the main controlling factors of debris flow triggering. More to the south, there is higher influence of altitude, aspect, and distance to faults. In all subsets, there is stronger influence of land use, geology, internal relief, and altitude as factors of debris flow triggering. Slope and planar curvature also play certain roles in the distribution of landslides. The lowest relations are observed in the case of profile curvature and aspect for the northern and central subsets.

The different influence of land use classes between the different subsets are probably caused by a much higher occurrence of bare land in the northern part than in the rest of the study area. In the central part the land use class of coniferous forests has a strong influence on landslide distribution. However this might be caused mainly by the lower altitudes of scarps in the central part. In the southern part about half of the debris flow source areas are located in the bare land class, and the influence of land use classes of shrubs, bushes and scarce vegetation is proportionally distributed. In the DF2001 database the bare land class has much higher occurrence than in the GeoIFFI database.

Distributions of scarps in the slope classes do not show any particular differences between the databases or between the subsets. Only in the southern subset, scarps are located on higher slope angles than in the northern and central subsets.

There is also a clear difference between the three parts in terms of aspect classes. In the northern part the scarps are located mainly on south and east facing slopes. The southern part has debris flow scarps distributed mostly in east and west directions. This is caused mostly by their presence near ridges with a north to south orientation. A strong difference was found between the GeoIFFI and DF2001 databases in the central subset. In the GeoIFFI database most of the scarps have a south facing orientation, while in the DF2001 database they are prevalently NW facing. This particular difference is caused by different spatial extent of the scarp. The scarps on the north facing slopes are larger than those on the south facing slopes.

In the northern part of Valtellina di Tirano, the debris flow scarps are located mainly in higher altitudes (more than 2,338 m a.s.l.), while in the southern part this correlation is not so obvious. Scarps in the central part are distributed on lower altitudes (from 1723 m a.s.l.) because the slopes adjacent to the main valley of the Adda River do not reach high altitudes.

Faults in the northern part of the study area do not show any significant correlation with debris flow triggering, but more to the south there is a higher influence of fault proximity on scarp occurrence. This could be partially explained by the proximity of the Insubric line and successive faults and thrusts. However, the main fault crossing the Adda Valley in the central part of the study area is mostly located in the floodplain. The differences in the distribution of debris flow scarps in the classes of internal relief, planar and profile curvatures and flow accumulation do not show any particular differences among the three regions. Scarps are located in classes of high internal relief as well as convex planar and profile curvatures, and low flow accumulation.

4.3. Comparison of random partition of the GeoIFFI and DF2001 inventories

The WofE modelling technique was applied several times with different combinations of the factor maps. For the first model all factor maps were used; the other models were built after removing less relevant factor maps based on the accountability and reliability indices (Table 2). SRCs were obtained using training subsets and PRCs were obtained using the validation subset. These subsets were generated by random, equal size (50%) subdivision of the inventories. Results of the best performing models are shown in Fig. 8 and Table 3. SRCs and PRCs from the DF2001 databases show slightly better results in terms of areas under curves, as compared to those from the GeoIFFI database.

Fig. 8 somewhere here

Table 3 somewhere here

The best performing model based on the GeoIFFI database is able to classify 80% of debris flow source areas in 30% of the territory with *AUC* (area under curve) of 84.04%. The model was made by combining altitude, land use, geology, slope, profile and planar curvature factor maps. The best model based on the DF2001 database shows slightly better results, which is able to classify more than 85% of the scarps in less than 30% of the area, with *AUC* being 86.54%. The best model generated from the DF2001 inventory was made by combining the altitude, land use, geology, slope and planar curvature factor maps.

AUC values for PRCs using the GeoIFFI database are slightly lower than those for SRCs, while for the DF2001 database this is reverse (Fig. 8 and Table 3). This result is very particular, because in general, SRCs should be located higher than PRCs, as SRCs are obtained using training subsets. In this case, the validation subset fits the model better than the training subset.

The use of DF2001 database gives better SRC and PRC results than the use of GeoIFFI database. This is most probably caused by the different purposes and ways of producing these databases. Debris flow scarps in the GeoIFFI database were mapped as points and are not always located in the correct place of the debris flow source. This inaccuracy is probably caused by the utilization of different sources of information for the fast generation of the GeoIFFI database for the whole Lombardy Region. On the other hand, scarps in the DF2001 database were mapped very carefully as polygons using stereoscopic air photo interpretation, followed by field surveys, with higher precision in scarp locations for the study area. The DF2001 database seems to better depict the debris flow source areas. However, this difference is not very spectacular, as the DF2001 inventory was mapped only for analysing debris flow susceptibility in the Valtellina di Tirano area while the GeoIFFI database was made for the whole Lombardy Region and for many landslide types.

4.4. Comparison of spatial partition of the GeoIFFI and DF2001 inventories

As can be seen from the accountability and reliability indices for both inventories, particular differences in debris flow sources exist within the study area. Results of the analysis of the best performing models for each subset are summarized in Fig. 9 and Table 4.

The spatially divided GeoIFFI inventory in terms of SRC shows better results than the randomly divided one; however, the PRC results for the randomly divided GeoIFFI inventory are better than those of the spatially divided subsets. The susceptibility models of all three subsets were always able to classify more than 70% of debris flow source areas in less than 20% of the whole territory. The best performing model was made using the southern subset with an *AUC* value of 89.51%. The best models for the northern and central subsets have *AUC*s of 87.88% and 84.48% respectively. Also PRCs for all three subsets are very similar, showing that the differences of the debris flow triggering conditions, among the subsets of the

GeoIFFI database, are not clearly captured by the database.

Much greater differences can be observed when comparing the results produced from the DF2001 inventory. The northern part of the study area clearly shows very particular conditions of debris flow triggering. The model, generated from the northern subset, was able to classify more than 90% of the scarps in less than 20% of the area with an *AUC* value of 92.88%. The results from the central and southern subsets were lower; nevertheless the *AUC* values always exceed 90% (91.75% and 90.96% for the central and southern subsets, respectively).

Fig. 9 somewhere here

Table 4 somewhere here

The differences in debris flow predisposing conditions among the northern, central and southern subsets could be also seen after obtaining PRCs for each subset (Fig. 10 and Table 5). Each map's prediction capability was tested by using the inventory dataset from the other parts of the study area (e.g. a PRC is obtained for the northern subset using the rest of the DF2001 database for the central and southern subsets; the differences in areas classified as susceptible could be seen). The results obtained from this cross-validation show the difference between causal factors affecting the debris flow triggering in each part of the study area. The differences in PRCs for the central and southern subsets are not very distinct. This means that factors contributing to debris flow triggering are more similar in the southern and central parts of the study area, and debris flows in the northern part have causal factors different from the rest of the region.

Fig. 10 somewhere here

Table 5 somewhere here

Final maps from the spatially divided inventories of the GeoIFFI and DF2001 databases were generated using the best performing combinations of the factor maps (in terms of SRC) for the three subsets of the spatially divided GeoIFFI and DF2001 databases (Fig. 9). Overlying these maps, we used the highest posterior probability values and then obtained SRCs, using one of the whole GeoIFFI and DF2001 databases. The results show that the spatially divided DF2001 model has an SRC with an *AUC* value of 89.01% and the model from the spatially divided GeoIFFI inventory has that of 85.06%. It can be concluded that the DF2001 inventory produced the best susceptibility map in terms of standard model performance.

4.5. Spatial pattern and main properties of the best performing susceptibility maps

All the best performing models show good and very similar results in terms of *AUC*. It was noticed, however, that the spatial pattern of the final maps differs. To quantify the differences between the maps, a four-class classification was applied using breakpoints at 10%, 30%, and 50% of the susceptible area (Fig. 11). Four maps corresponding to the four classes were obtained and simply overlaid using the Rank Difference tool of the Spatial Data Modeller (Sawatzky et al., 2008). Percentages of correspondence between the classes of the susceptibility maps are shown in Table 6. The lowest difference in spatial distribution was found between the maps produced by the randomly divided GeoIFFI and DF2001 inventories (81.11% correspondence), while the highest difference was found between the maps from the spatially divided DF2001 inventory and the randomly divided GeoIFFI inventory (70.80%

correspondence). These results might have important consequence in choosing the correct model representing the occurrence of the debris flow source areas. To analyse this problem, the percentage of landslide sources in particular classes were calculated together with the landslide density (Table 7). It can be seen from the table that the landslide percentages and densities decrease gradually from the very high to low susceptible classes in all maps. The model which allowed us to classify most debris flow sources in the very high class was made by the combination of the best northern, central, and southern subsets of the DF2001 database. More than 63% of debris flow sources from the DF2001 database fall into less then 10% of the most susceptible area. The DF2001 database shows in both cases better results than the GeoIFFI database. In the GeoIFFI database much more debris flow sources fall into the less susceptible half of the study area (4.13% and 5.82% respectively), as compared to the DF2001 where only 1.17% and 1.56% of debris flow sources belong to 50% of less susceptible area.

Fig. 11 somewhere here

Table 6 somewhere here

Table 7 somewhere here

To evaluate if the DF2001 inventory is a better input for landslide susceptibility mapping than the GeoIFFI inventory, a cross-validation was performed. The DF2001 inventory was used to calculate PRCs of the best map produced by the GeoIFFI inventory. The *AUC* value of the PRC for the map generated from the randomly divided GeoIFFI inventory reached 86.28%, which is higher than that of the SRC of this map (85.74%). This situation leads to a simple conclusion that the GeoIFFI inventory might be enough for producing a reliable susceptibility map. However, the mismatch of almost 30% in the spatial pattern of the maps produced from these inventories does not provide a simple conclusion (Table 6). The good performance of the map produced from the GeoIFFI inventory could be caused by the high influence of important factor map classes (slope, land use, geology, internal relief, and planar curvature; Table 1). It should be noted that the use of standard evaluation techniques (SRCs, PRCs) has a significant drawback in that it does not take into account the loss of spatial information. As a consequence, compared maps can show very similar values of *AUC*, but their spatial pattern can be highly different.

4.6. Final susceptibility map

The resulting susceptibility map with the best potential to predict future landslide-induced debris flow source areas was made from the combination of maps from the spatially divided DF2001 database with the highest *AUC* values of SRCs. The final map has an *AUC* value of 89.01% for the SRC, which is good compared to the first application of the randomly divided DF2001 database (*AUC* for the SRC was 87.16%). Moreover this map better captures the differences in debris flow sources in different parts of the study area. The final susceptibility map was reclassified into five classes, according to the percentage of debris flow scarps that fall into particular susceptibility classes. Breakpoints were put at 75%, 85%, 95%, and 99% of the landslide scarps (Fig. 12 and Table 8). The extent of the very high susceptibility class is 14.52% of the study area, and more than a half of the study area (52.99%) belongs to the very low or non-susceptible class. Also the density of debris flow scarps decreases from very high to very low susceptibility values (Fig. 13).

Fig. 12 somewhere here

Table 8 somewhere here

Fig. 13 somewhere here

Moreover, when applying the same classification to the best maps using the randomly divided GeoIFFI and DF2001 databases, there is significant improvement in the restriction of the area classified as very highly susceptible. In the case of the GeoIFFI database, 75% of debris flow scarps lie within 19.10% of the area; and only 45.80% of the area is classified as very low susceptible. The randomly divided DF2001 database has better results, when 75% of debris flow scarps lie within 18.70% of the area and 48.20% of the area is classified as very low susceptible. Comparison with the best map from the spatially divided GeoIFFI inventory shows even higher differences, when the GeoIFFI map has only 39.41% of the area classified as very low susceptible and the highest class covers 19.37% of the area.

4.7. Limitations of susceptibility modelling

First limitation of the statistically based landslide susceptibility modelling is connected with the fact that the landslide inventory is based on information from specific time and the produced susceptibility map shows only the landslide susceptibility for this particular moment. Another limitation arises from different spatial and temporal resolution of input factor maps. In this case, maps of the same resolution should be used as in the case of this study. Data mining procedures (as accountability and reliability indices) might be useful for supporting expert knowledge about the causal factors of landslide triggering. However, the use of such simple indices has a lot of limitations when important information on the particular classes of the causative factor maps is not taken into account.

If the susceptibility maps are well made and evaluated, they could significantly contribute to the public safety in endangered areas. Nevertheless, in the case of automatically calculated maps, their meaning highly depends on the combination of factor maps used as inputs of the analysis. Moreover, it is certain, that high knowledge of the studied territory is essential for the calculation of landslide susceptibility maps. Skills in model calibration alone are not enough to obtain good and reliable results. Thus, an expert knowledge of the territory as well as the landslides is crucial for assessing the credibility of automatically calculated models. It was demonstrated that even within a relatively small area the triggering conditions of debris flows could be highly variable. Therefore, it is better not to perform statistical analysis over a large area because particular differences in susceptibility conditions are not shown. Capturing specific conditions of landslide sources for a large area may be possible if an inventory is divided into sub-inventories with different subtypes of a particular landslide type.

In the case of debris flow susceptibility mapping, the correct delimitation of susceptible areas is still the first step of hazard analysis, because runout analysis has to be performed subsequently. The step is important, however, because the runout analysis is difficult to perform when the delimitation of the susceptible areas is unclear and debris flow volumes are not quantified.

5. Conclusions

A lot of developments have been made in indirect statistically based landslide hazard mapping on medium scale (1:25 000 to 1:50 000) in recent years. Nevertheless, still many limitations exist. One of them is the availability and completeness of landslide inventory databases, which are used for computation of susceptibility and hazard models. Even if landslide inventories are available, they still can have a lot of problems such as inaccuracy and the lack of sufficient temporal information. Available temporal data, if any, would allow us to analyse the frequency and magnitude of landslides for a quantitative risk assessment.

The comparison between the official database (GeoIFFI) and the recently mapped inventory (DF2001) did not show marked differences in the importance of particular factor classes, when those inventories were randomly subdivided. The differences between the inventories arise when they were spatially subdivided into three parts in order to capture peculiar triggering factors for each part. In that case no particular differences in the model performance were observed in the GeoIFFI database. On the contrary, the DF2001 database was able to capture these differences. It is advisable to divide a region into environmentally different subsets to better capture the peculiar characteristics of landslide controlling factors. The final susceptibility map was made by combining the models from the spatially divided DF2001 inventory. This final map has five classes according to the percentage of debris flow scarps. The improvement of model performance using the DF2001 inventory could be caused by more complete representation of the landslides in the DF2001 inventory.

The improvement in model performance is different from the findings of Poli and Sterlacchini (2007). They analyzed representation strategies of landslide scarps in susceptibility studies, and found that different density of cells used to represent landslide scarps did not greatly influence the posterior probability maps. This dissimilarity probably reflects different types of landslides analysed (translational and rotational landslides) and different spatial extents of scarp areas. Moreover, Poli and Sterlacchini (2007) analysed only one inventory of landslides represented as points, while this study compared two different inventories, one mapped with points and the other mapped with polygons.

This study shows that the produced susceptibility maps depend on the landslide inventories used as input, and the spatial pattern of the maps produced using different inventories varies a lot, although this difference does not large when standard evaluation techniques are applied. The spatial distribution of susceptible areas in the best performing maps disagrees by 20% to 30%. The results of this study have significant implications for landslide assessment in which susceptibility maps at medium scales are often used.

Acknowledgements

The authors would like to thank Dr. Jean-Philippe Malet and Dr. Gary L. Raines for their comments which improved the paper. This research was supported by the EC 6th Framework Project “Mountain Risks” and Marie Curie Research & Training Network (http://mountain-risks.eu) in which the authors are involved.

ACCEPTED MANUSCRIPT

References

Agterberg, F.P., Bonham-Carter, G.F., Wright, D.F., 1989. Weights of Evidence modelling: a new approach to mapping mineral potential. In: Agterberg, F.P., Bonham-Carter, G.F. (Eds.), Statistical Applications in the Earth Sciences. Geological Survey of Canada, Paper 89-9, pp. 171-183.

Beguería, S., 2006. Validation and evaluation of predictive models in hazard assessment and risk management. Natural Hazards 37, 315-329.

Bonham-Carter, G.F., 1994. Tools for map pairs. In: Merriam, D.F. (Ed.), Geographic Information Systems for Geoscientists, Pergamon Press, Oxford, pp. 221-265.

Bonham-Carter, G.F., 1996. Geographic Information Systems for Geoscientists: Modeling with GIS. Pergamon, Elsevier Science Ltd.

Bonham-Carter, G.F., Agterberg, F.P., Wright, D.F., 1988. Integration of geological datasets for gold exploration in Nova Scotia. Photogrammetric Engineering 54, 1585-1592.

Cancelli, A., Nova, R., 1985. Landslides in soil debris cover triggered by rainstorm in Valtellina (Central Alps, Italy). Proceedings of 4th International Conference and Field Workshop on Landslides, Tokyo, Japan, pp. 262-267.

CARG Project, 1992. The New Italian 1:50 000 Geological Map. National Geological Survey, Rome, Italy.

Carrara, A., Cardinali, M., Detti, R., Guzzetti, F., Pasqui, V., Reichenbach, P., 1991. GIS Techniques and statistical models in evaluating landslide hazard. Earth Surface Processes and Landforms 16, 427-445.

Carrara, A., Cardinali, M., Guzzetti, F., Reichenbach, P., 1995. GIS technology in mapping landslide hazard. In: Carrara, A., Guzzetti, F. (Eds.), Geographical Information Systems in Assessing Natural Hazards, Kluwer Academic Publisher, Dordrecht, pp. 135-176.

Carrara, A., Crosta, G., Frattini, P., 2008. Comparing models of debris flow susceptibility in the alpine environment. Geomorphology 94, 353-378.

Castellanos Abella, E.A., 2008. Provincial landslide risk assessment. In: Castellanos Abella, E.A., Multi-scale landslide risk assessment in Cuba, Utrecht University, Utrecht, ITC Dissertation 154, pp. 101-152.

Chung, C.-J., Fabbri, A.G., 1999. Probabilistic prediction models for landslide hazard mapping. Photogrammetric Engineering and Remote Sensing 65, 1389-1399.

Chung, C.-J., Fabbri, A.G., 2003. Validation of spatial prediction models for landslide hazard mapping. Natural Hazards 30, 451-472.

Chung, C.-J., Fabbri, A.G., 2008. Predicting landslides for risk analysis – spatial models tested by a cross-validation technique. Geomorphology 94, 438-452.

Crosta, G., 1990. A study of slope movements caused by heavy rainfall in Valtellina (July 1987), Proceedings of 6th IVCFL, Milan, pp. 247-258.

Crosta, G., Marchetti, M., Guzzetti, F., Reichenbach, P., 1990. Morphological classification of debris-flow processes in South-Central Alps (Italy). Proceedings of 6th International IAEG Congress, Amsterdam, The Netherlands, pp. 1565-1572.

Crosta, G.B., Dal Negro, P., Frattini, P., 2003. Soil slips and debris flows on terraced slopes. Natural hazards and Earth System Sciences 3, 31-42.

DUSAF Project, 2003. Destinazione d'Uso dei Suoli Agricoli e Forestali, Lombardy Region, Milano, Italy.

Fell, R., Corminas, J., Bonnard, C., Cascini, L., Leroi, E., Savage, W.Z., 2008. Guidelines for landslide susceptibility, hazard and risk zoning for land-use planning. Engineering Geology 102, 99-111.

GeoIFFI, 2006. The Regional Inventory (1:10 000) of Landslides and Hydrogeological Events, Lombardy Region, Italy [www.cartografia.regione.lombardia.it/GeoIFFI].

Greenbaum, D., Bowker, M.R., Dau, I., Bropsy, H., Greally, K.B., McDonald, A.J.W., Marsh, S.H., Northmore, K.J., O`Connor, E.A., Prasad, S., Tragheim, D.G., 1995a. Rapid Methods of Landslide Hazard Mapping: Fiji Case Study. Technical Report WC/95/28, British Geological Survey (BGS), Natural Environmental Research Council, Keyworth, Nottingham.

Greenbaum, D., Tutton, M., Bowker, M.R., Browne, T.J., Buleka, J., Greally, K.B., Kuna, G., McDonald, A.J.W., Marsh, S.H., O`Connor, E.A., Tragheim, D.G., 1995b. Rapid Methods for Landslide Hazard Mapping: Papua New Guinea Case Study. Technical Report WC/95/27, British Geological Survey (BGS), Natural Environmental Research Council, Keyworth, Nottingham.

Guzzetti, F., Crosta, G., Marchetti, M., Reichenbach, P., 1992. Debris flows triggered by the July, 17-19, 1987 strom in the Valtellina area (Northern Italy). International Symposium Interpraevent 1992, Bern, Switzerland, pp. 193-203.

Guzzetti, F., Cardinali, M., Reichenbach, P., 1994. The AVI Project: A bibliographical and archive inventory of landslides and floods in Italy. Environmental Management 18, 623-633.

Guzzetti, F., Carrara, A., Cardinali, M., Reichenbach, P., 1999. Landslide hazard evaluation: a review of current techniques and their application in a multi-scale study, Central Italy. Geomorphology 31, 181-216.

Guzzetti, F., Galli, M., Reichenbach, P., Ardizzone, F., Cardinali, M., 2006a. Landslide hazard assessment in the Collazone area, Umbria, Central Italy. Natural Hazards and Earth System Sciences 6, 115-131.

Guzzetti, F., Reichenbach, P., Ardizzone, F., Cardinali, M., Galli, M., 2006b. Estimating the quality of landslide susceptibility models. Geomorphology 81, 166-184.

ITC, 2009. ILWIS - Remote Sensing and GIS software: Integrated Land and Water Information System. [http://www.itc.nl/Pub/Home/Research/Research_output/ILWIS_-_Remote_Sensing_and_GIS_software.html].

Lombardy Region, 2002. Inventario delle frane e dei dissesti idrogeologici della Regione Lombardia. Direzione generale territorio e urbanistica. Struttura rischi idrogeologici, Milano, 2 CD-ROM.

Poli, S., Sterlacchini, S., 2007. Landslide representation strategies in susceptibility studies using Weights-of-Evidence modeling technique. Natural Resources Research 16, 121-134.

Raines, G., 1999. Evaluation of weights of evidence to predict epithermal-gold deposits in the great basin of western United States. Natural Resources Research 8, 257-276.

Raines, G. L., Bonham-Carter, G. F., Kamp, L., 2000. Predictive Probabilistic Modeling Using ArcView GIS. ArcUser 3, 45-48.

Remondo, J., Bonachea, J., Cendrero, A., 2005. A statistical approach to landslide risk modelling at basin scale: from landslide susceptibility to quantitative risk assessment. Landslides 2, 321-328.

Sawatzky, D.L., Raines, G.L., Bonham-Carter, G.F., Looney, C.G., 2008. Spatial Data Modeller (SDM): ArcMAP 9.2 geoprocessing tools for spatial data modelling using weights of evidence, logistic regression, fuzzy logic and neural networks. [http://arcscripts.esri.com/details.asp?dbid=15341].

Schuster, R.L., 1996. Socio-economic significance of landslides. In: Turner, A.K., Schuster, R.L. (Eds.), Landslide Investigation and Mitigation: Transportation Research Board, Specific Report, 247, National Academy Press, Washington, pp. 12-35.

Soeters, R., van Westen, C.J., 1996. Slope instability: recognition, analysis and zonation. In: Turner, A.K., Schuster, R.L. (Eds.), Landslides Investigation and Mitigation: Transportation Research Board, Specific Report, 247, National Academy Press, Washington, pp. 129-177.

Süzen, M.L., Doyuran, V., 2004. Data driven bivariate landslide susceptibility assessment using geographical information systems: method and application to Asarsuyu catchment, Turkey. Engineering Geology 71, 303–321.

Thiery, Y., Malet, J.-P., Sterlacchini, S., Puissant, A., Maquaire, O., 2007. Landslide susceptibility assessment by bivariate methods at large scales: Application to a complex mountainous environment. Geomorphology 92, 38-59.

van Westen, C.J., 1993. Application of Geographic Information Systems to Landslide Hazard Zonation. ITC Publication, 15. International Institute for Aerospace and Earth Resources Survey (ITC), Enschede.

van Westen, C.J., Rengers, N., Soeters, R., 2003. Use of geomorphological information in indirect landslide susceptibility assessment. Natural Hazards 30, 399–419.

Figures

Fig. 1. Simplified geomorphological map of the study area of the Consortium of Mountain Municipalities of Valtellina di Tirano. The location of the study area in the Lombardy Region and in Italy is shown on the right.

Fig. 2. Photographs of debris flow scarps in the study area. A: debris flow scarp in the Val Grosina Valley in highly fractured gneiss; B: Scarp in moraine deposits in the central part of the study area; C: debris flow in unconsolidated colluvial sediments in the Val Belviso Valley. Locations of the photos are shown in Fig. 3.

Fig. 3. Three subdivisions of the debris flow inventories. 1□3: Locations of the scarps in Fig. 2. Rectangle shows the extent of Fig. 5.

Fig. 4. Flowchart of the applied methodology.

Fig. 5. Scheme showing the generation of the new DF2001 database.

Fig. 6. Ten factor maps used in the WofE analysis. A – altitude, B – aspect, C – distance to faults, D – internal relief, E – land use, F – geology, G – planar curvature, H – profile curvature, I – slope, J – flow accumulation. Land use and geology factor maps are generalised and re-classified. BAL: Bare land, SCV: Scarce vegetation, SAB: Shrubs and bushes, FOR: Forests, GRA: Grassland, CRO: Crops, URB: Urban fabric, WAT: Water courses, COL: Colluvial sediments, MIC: Micaschists, INT: Intrusive rocks, SED: Sedimentary rocks, GNE: Gneiss, MOR: Moraine deposits, QUA: Quartzite OTR: Other rock

types.

Fig. 7. Main debris flow characteristics for each database and subset. Geological classes are generalised.

Fig. 8. Comparison of success and prediction rate curves (SRC and PRC) generated for models with the best results for the GeoIFFI and DF2001 databases and random partition of the inventories.

Fig. 9. Comparison of success rate curves (SRCs) generated for models with the best results for the GeoIFFI and DF2001 databases and spatial partition of the inventories.

Fig. 10. Comparison of prediction rate curves (PRCs) generated for models with the best results for the GeoIFFI and DF2001 databases and spatial partition of the inventories.

Fig. 11. Example of spatial difference among four best models generated using different inventory subsets. Rectangle shows the location of the enlarged area. Corresponding inventories are superimposed over the enlarged area. VH – very high susceptibility; H – high susceptibility, M – medium susceptibility, L – low susceptibility.

Fig. 12. Success rate curve (SRC) of the final susceptibility map. The susceptibility classes from left to right are: very high, high, medium, low, very low, and not susceptible.

Fig. 13. Final susceptibility map with debris flow scarps of the DF2001 inventory superimposed. VH – very high susceptibility; H – high susceptibility, M – medium susceptibility, L – low susceptibility, VL – very low or no susceptibility.

Tables

Table 1. Highest and lowest classes of debris flow scarp densities for the five most relevant factors.

Table 2. Accountability (*A*) and reliability (*R*) for the different factor maps and different subsets used in the analysis. The most important factors and the highest accountability and reliability indices for each subset map are highlighted in bold.

Table 3. *AUC* values of success and prediction rate curves (SRC and PRC) generated for models with the best results for the GeoIFFI and DF2001 databases and random partition of the inventories.

Table 4. *AUC* values of success rate curves (SRC) generated for models with the best results for the GeoIFFI and DF2001 databases and spatial partition of the inventories.

Table 5. *AUC* values of prediction rate curves (PRC) generated for models with the best results for the GeoIFFI and DF2001 databases and spatial partition of the inventories

Table 6. Percentage of correspondence in classification between the best susceptibility maps generated from randomly (R) and spatially (S) divided GeoIFFI and DF2001 inventories. Maps were classified into four classes according to the percentage of susceptible area using breakpoints at 10%, 30% and 50%.

Table 7. Densities and percentage of debris flow sources in the best maps for the GeoIFFI and DF2001 inventories made by random or spatial subdivision. Maps were classified into four classes according to the percentage of susceptible area using breakpoints at 10%, 30% and 50%.

Table 8. Debris flow source areas densities and percentage according to the DF2001 inventory database for the classes of the final susceptibility map.

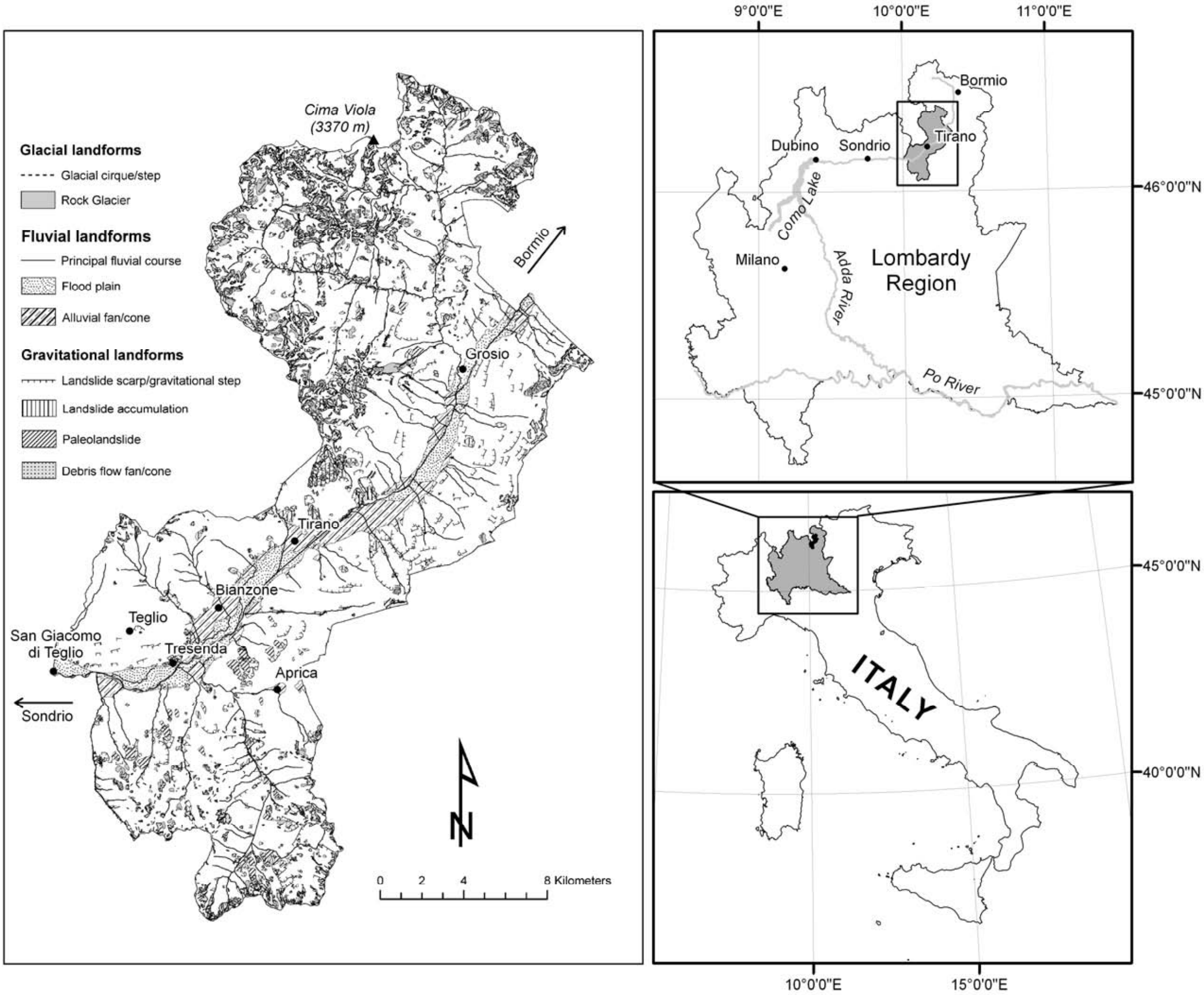

Fig. 1

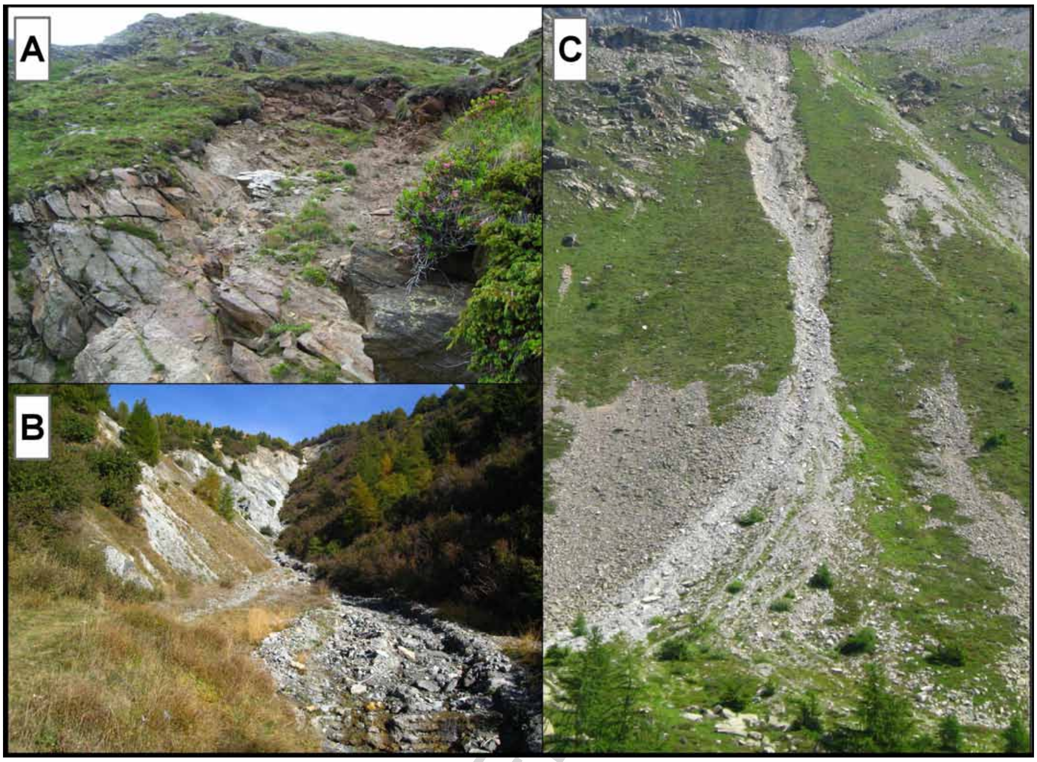

Fig. 2

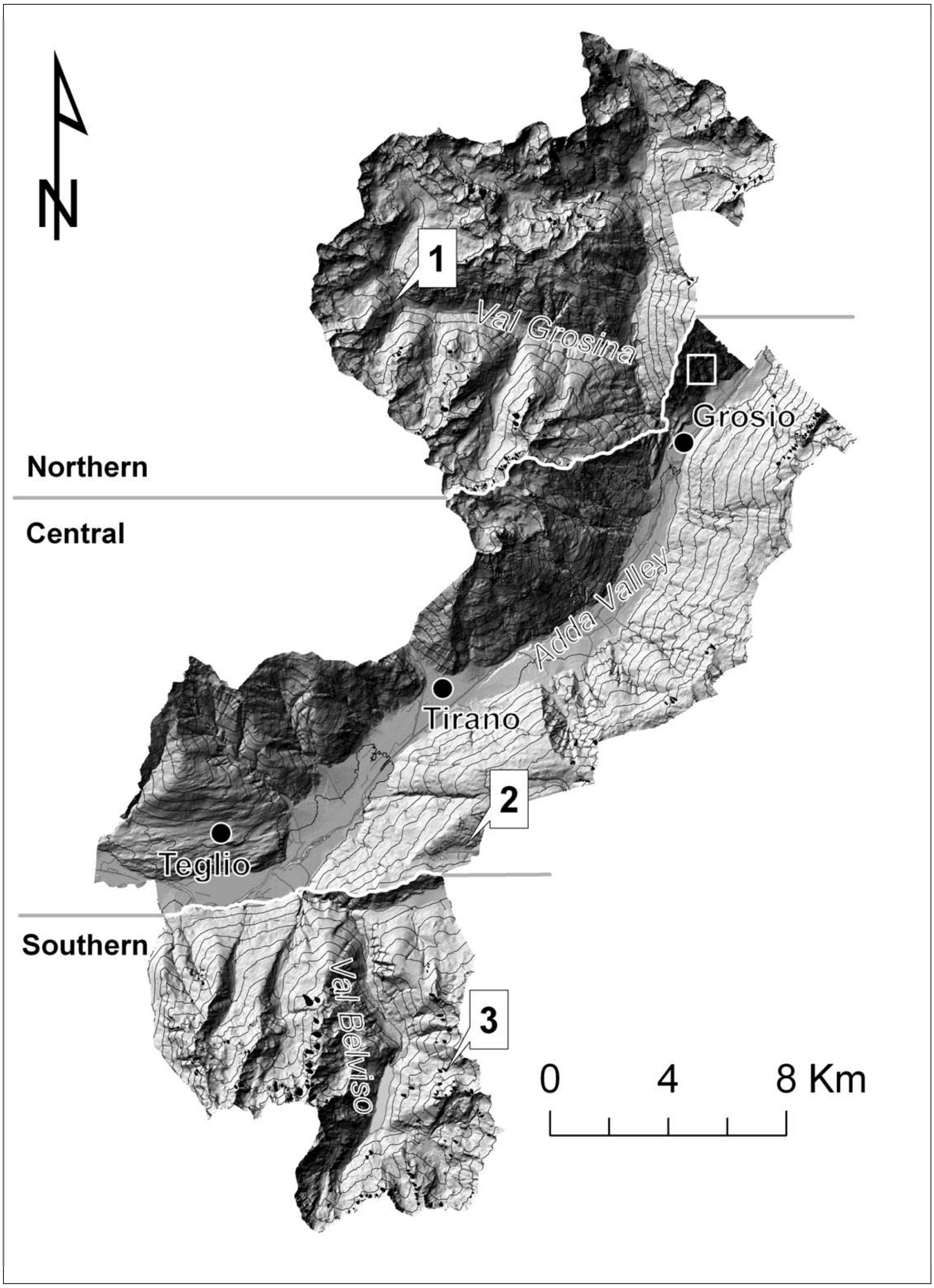
N
1
Val Grosina
Grosio
Northern
Central
Adda Valley
Tirano
2
Teglio
Southern
Val Belviso
3
0
4
8 Km

Fig. 3

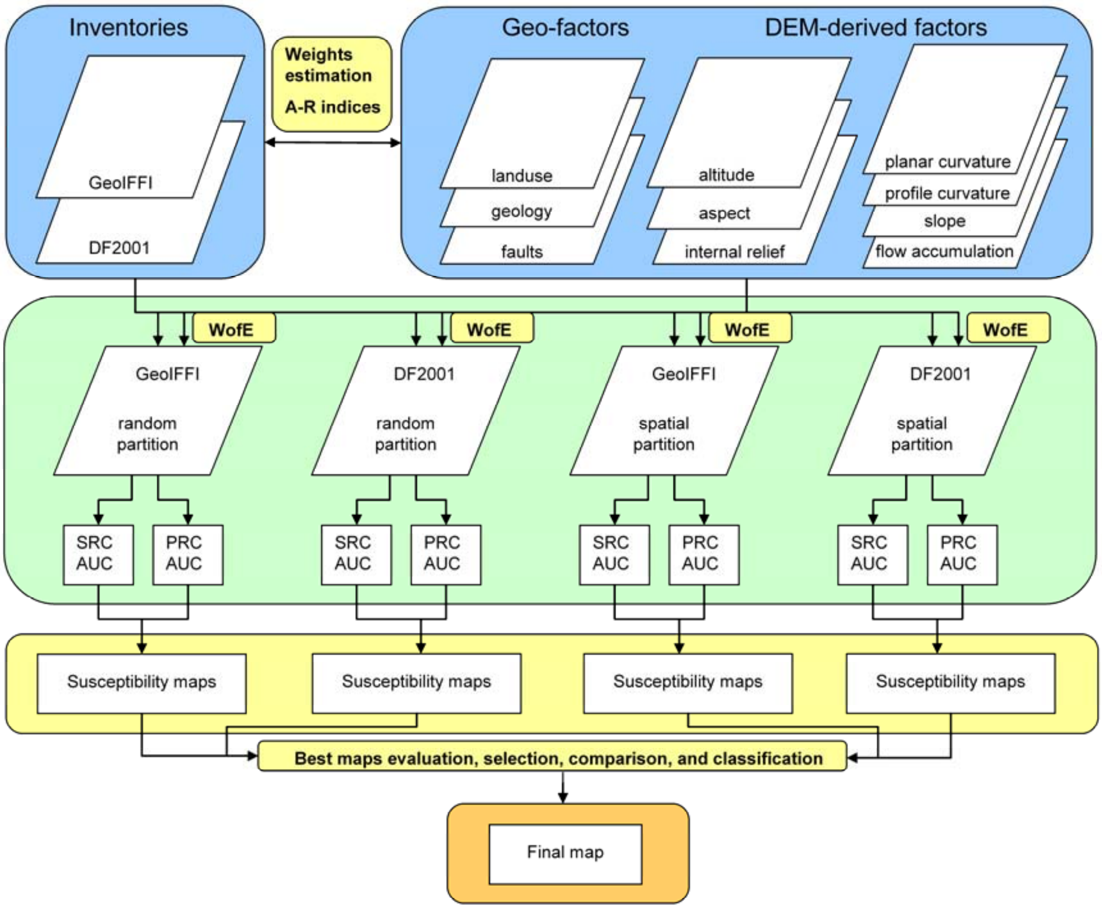

Inventories
GeoIFFI
DF2001
Weights estimation
A-R indices
Geo-factors
DEM-derived factors
landuse
geology
faults
altitude
aspect
internal relief
planar curvature
profile curvature
slope
flow accumulation
WofE
WofE
WofE
WofE
GeoIFFI
random partition
DF2001
random partition
GeoIFFI
spatial partition
DF2001
spatial partition
SRC AUC
PRC AUC
SRC AUC
PRC AUC
SRC AUC
PRC AUC
SRC AUC
PRC AUC
Susceptibility maps
Susceptibility maps
Susceptibility maps
Susceptibility maps
Best maps evaluation, selection, comparison, and classification
Final map

Fig. 4

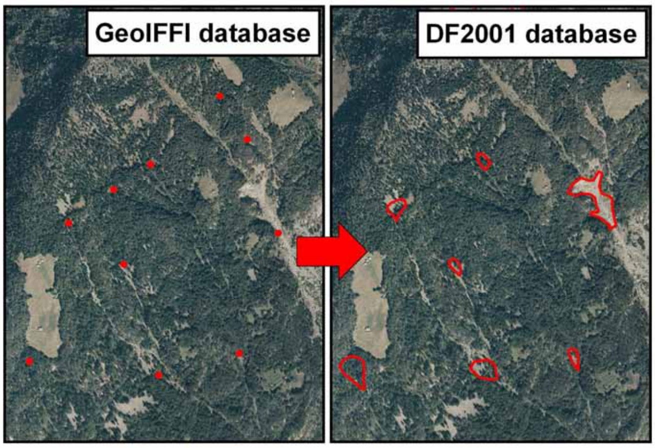

GeoIFFI database
DF2001 database

Fig. 5

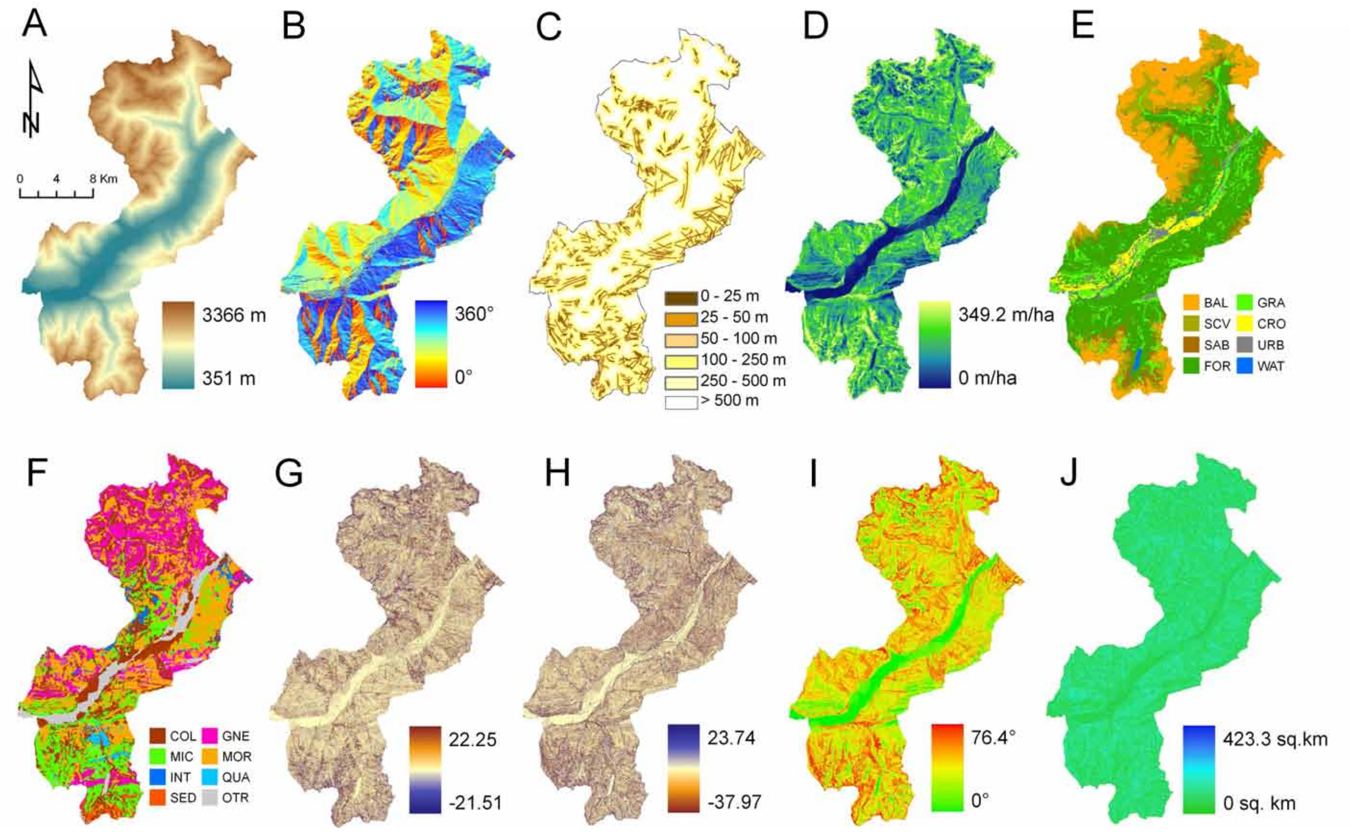

A
B
C
D
E
0 4 8 Km
3366 m
351 m
360°
0°
0 - 25 m
25 - 50 m
50 - 100 m
100 - 250 m
250 - 500 m
> 500 m
349.2 m/ha
0 m/ha
BAL
GRA
SCV
CRO
SAB
URB
FOR
WAT
F
G
H
I
J
COL
GNE
MIC
MOR
INT
QUA
SED
OTR
22.25
-21.51
23.74
-37.97
76.4°
0°
423.3 sq.km
0 sq. km

Fig. 6

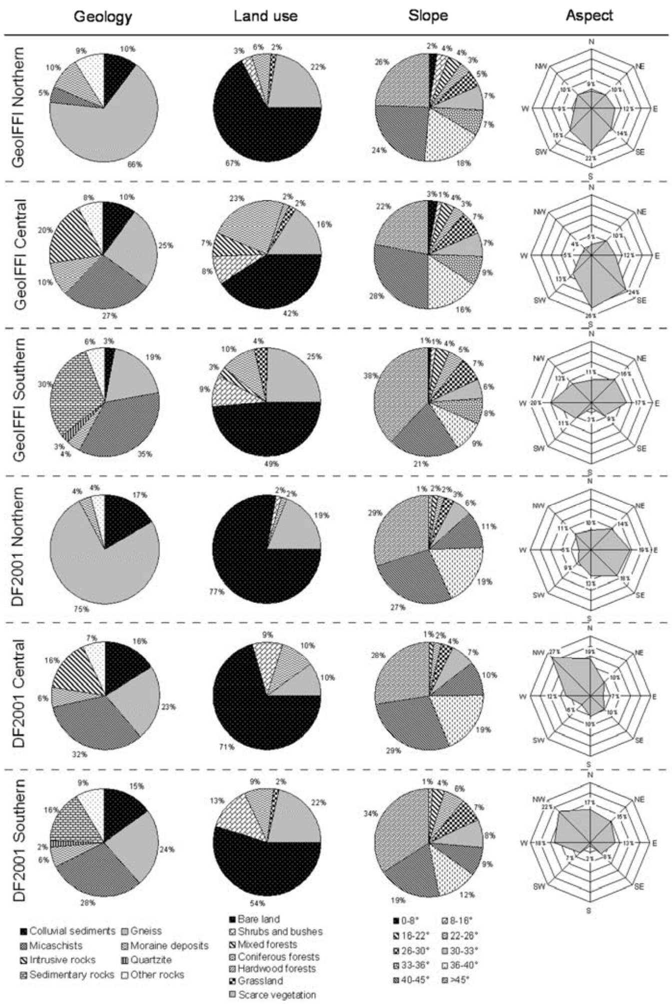
Geology
Land use
Slope
Aspect
GeoIFFI Northern
GeoIFFI Central
GeoIFFI Southern
DF2001 Northern
DF2001 Central
DF2001 Southern
Colluvial sediments
Gneiss
Micaschists
Moraine deposits
Intrusive rocks
Quartzite
Sedimentary rocks
Other rocks
Bare land
Shrubs and bushes
Mixed forests
Coniferous forests
Hardwood forests
Grassland
Scarce vegetation
0-8°
8-16°
16-22°
22-26°
26-30°
30-33°
33-36°
36-40°
40-45°
>45°

Fig. 7

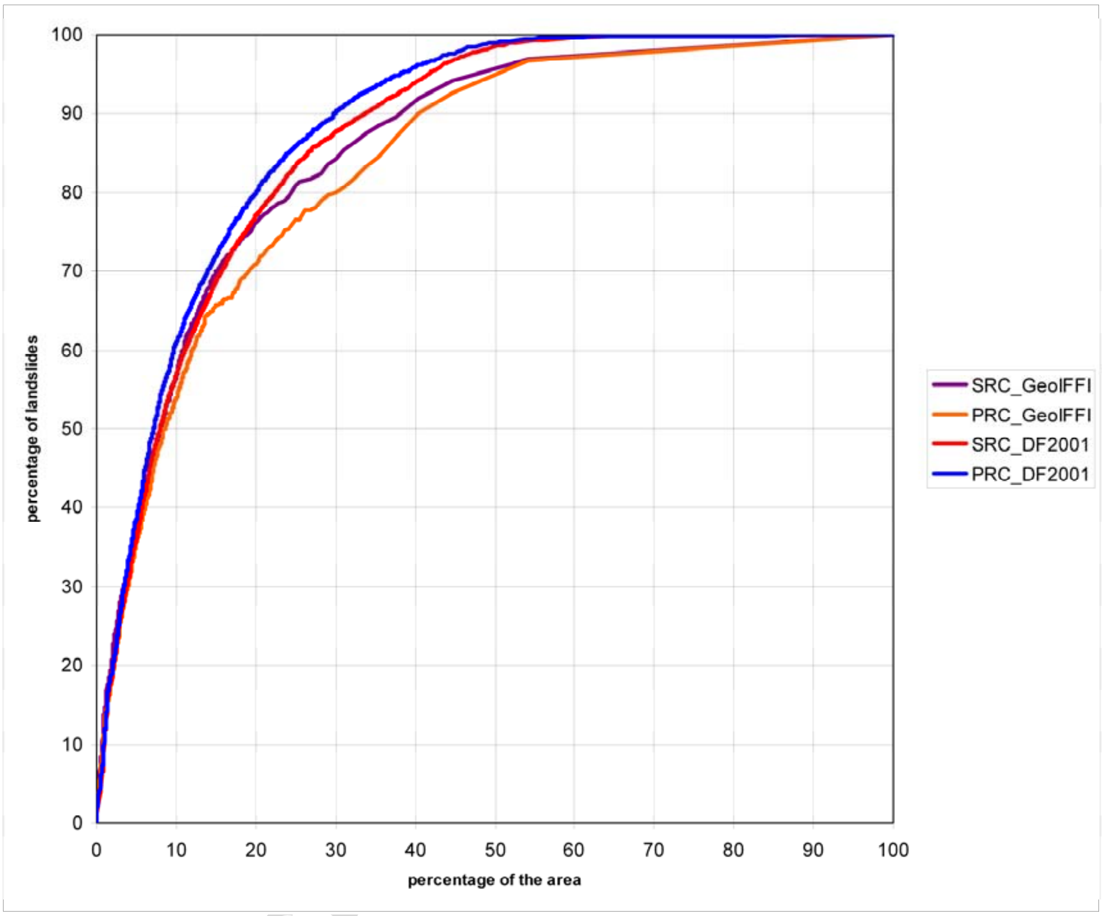

100
90
80
70
60
50
40
30
20
10
0
percentage of landslides
0
10
20
30
40
50
60
70
80
90
100
percentage of the area
SRC_GeoIFFI
PRC_GeoIFFI
SRC_DF2001
PRC_DF2001

Fig. 8

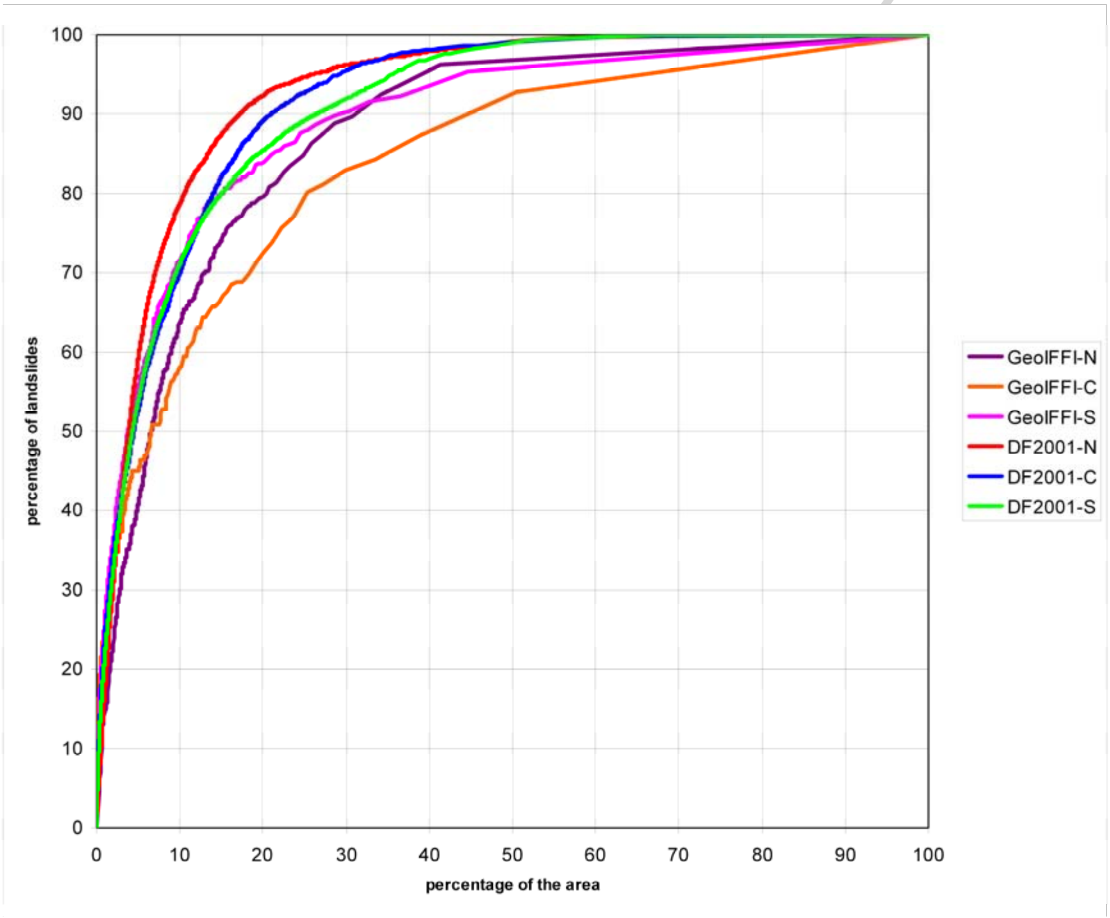

percentage of landslides
100
90
80
70
60
50
40
30
20
10
0
0
10
20
30
40
50
60
70
80
90
100
percentage of the area
GeoIFFI-N
GeoIFFI-C
GeoIFFI-S
DF2001-N
DF2001-C
DF2001-S

Fig. 9

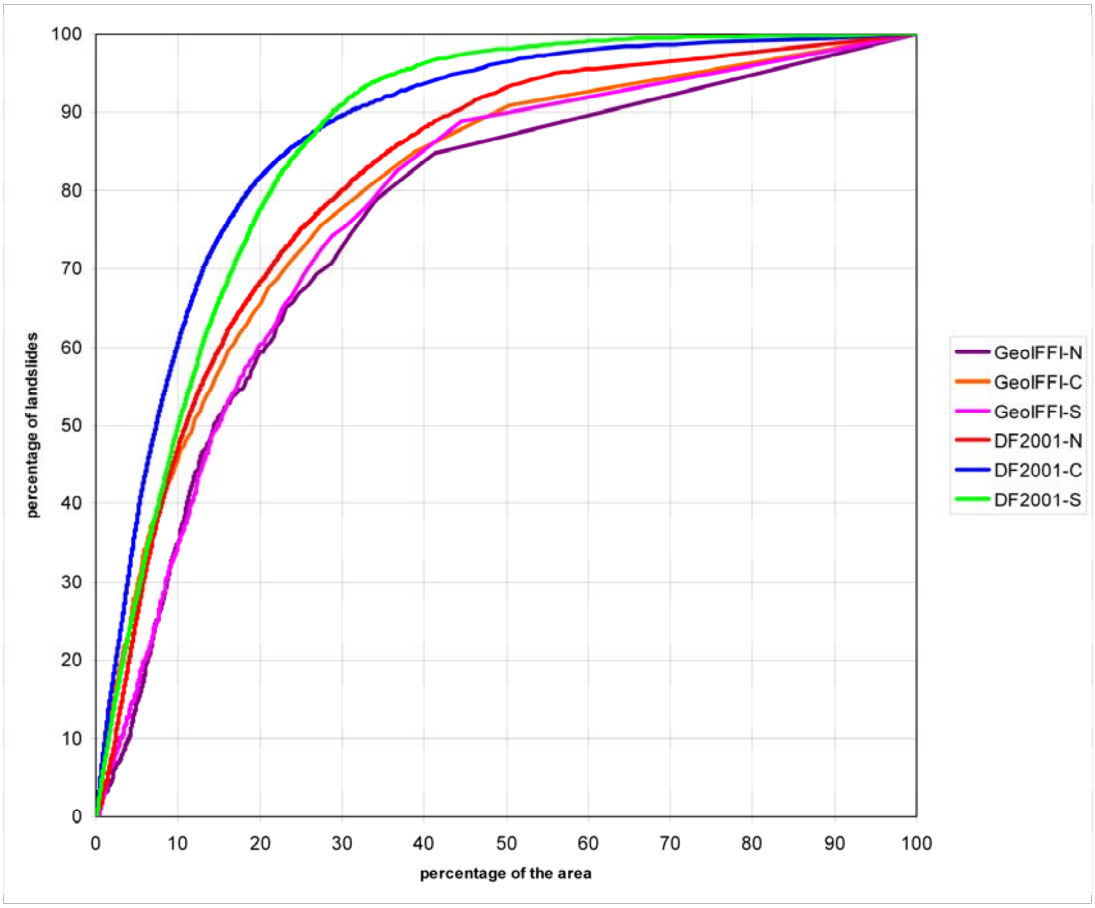

100
90
80
70
60
50
40
30
20
10
0
percentage of landslides
0
10
20
30
40
50
60
70
80
90
100
percentage of the area
GeoIFFI-N
GeoIFFI-C
GeoIFFI-S
DF2001-N
DF2001-C
DF2001-S

Fig. 10

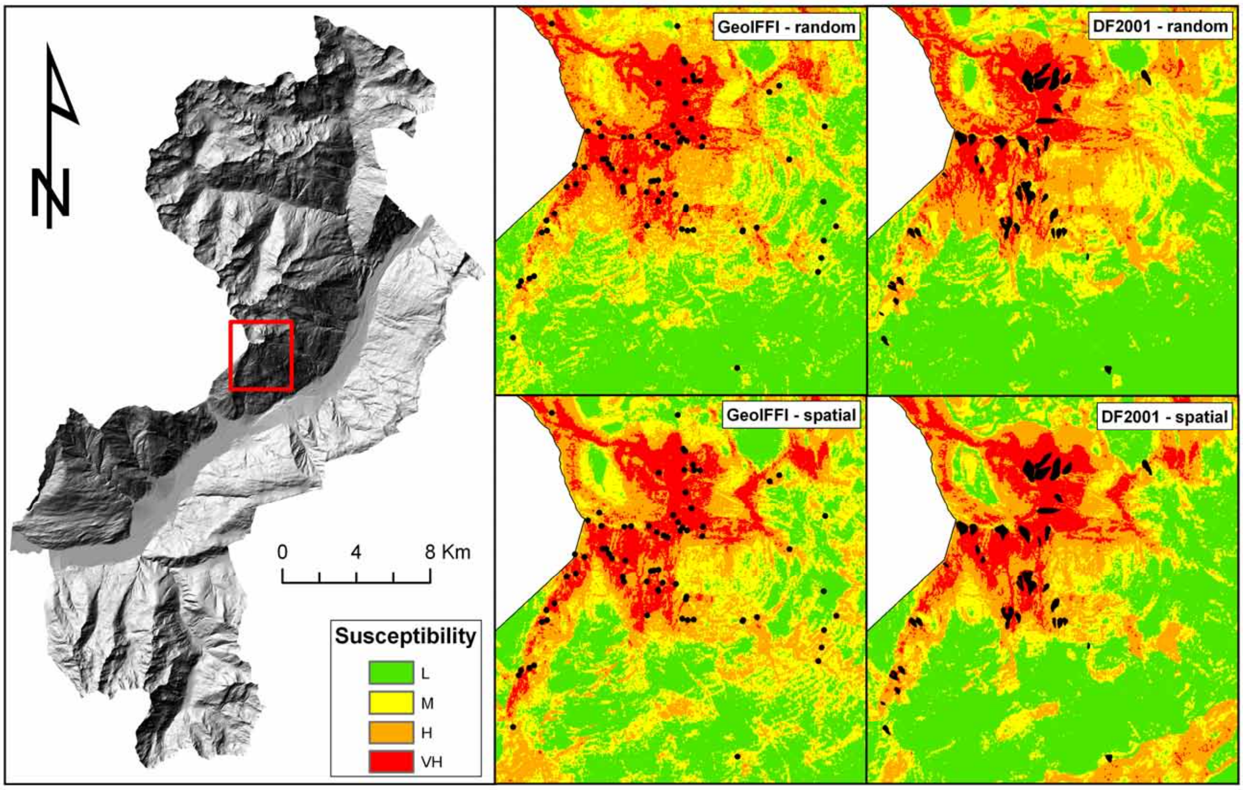
GeoIFFI - random
DF2001 - random
GeoIFFI - spatial
DF2001 - spatial
0
4
8 Km
Susceptibility
L
M
H
VH

Fig. 11

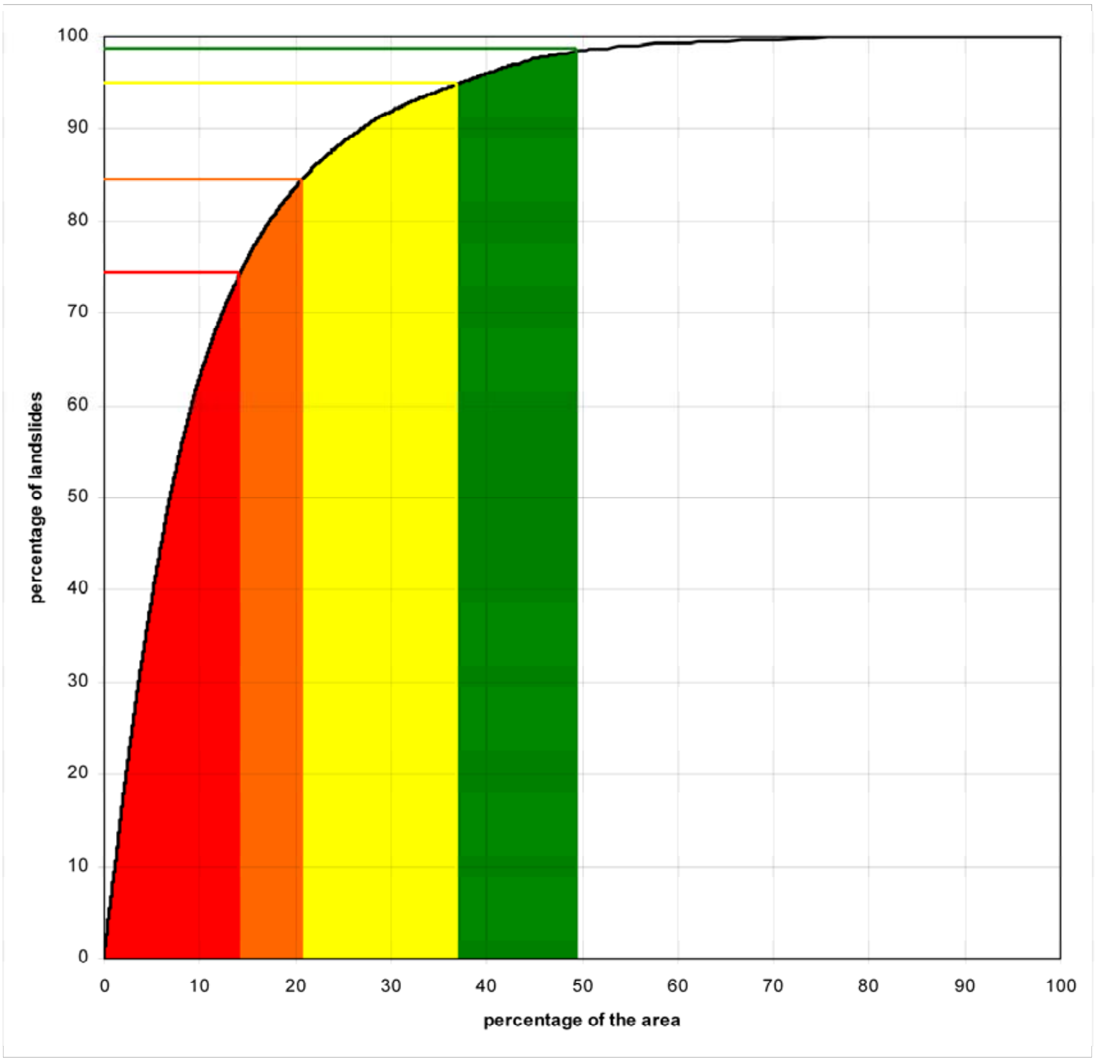

100
90
80
70
60
50
40
30
20
10
0
percentage of landslides
0
10
20
30
40
50
60
70
80
90
100
percentage of the area

Fig. 12

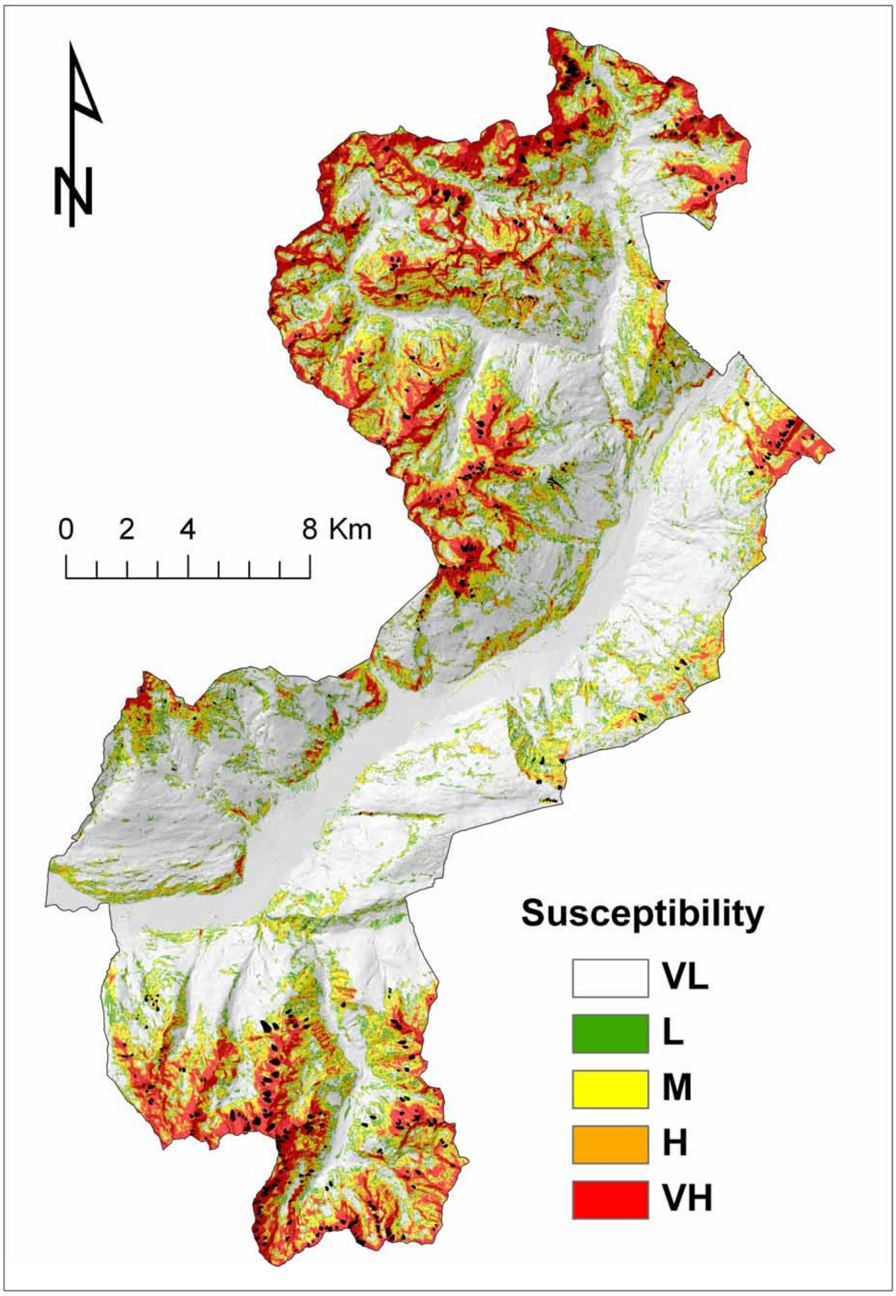

Fig. 13

	GeoIFFI factor map class	GeoIFFI density	DF2001 factor map class	DF2001 density
Slope (°)	44.9 - 76.4	0.001100	44.9 - 76.4	0.033668
highest classes	39.8 - 44.9	0.000792	39.8 - 44.9	0.023910
	36.2 - 39.8	0.000434	36.2 - 39.8	0.014894
	22.2 - 26.4	0.000130	16.5 - 22.2	0.002387
lowest classes	8.1 - 16.5	0.000073	8.1 - 16.5	0.000764
	0 - 8.1	0.000055	0 - 8.1	0.000095
Landuse	Bare land	0.000891	Bare land	0.031782
highest classes	Vegetation on rocks	0.000568	Shrubs and bushes	0.014225
	Reforested areas	0.000533	Vegetation on rocks	0.013478
	Pastures	0.000109	Pastures	0.001037
lowest classes	Mixed forests	0.000078	Mixed forests	0.000325
	Broadleaf forests	0.000031	Broadleaf forests	0.000107
Geology	Sandstones	0.005285	Sandstones	0.086039
highest classes	Claystones	0.004514	Claystones	0.072444
	Conglomerate outcrops	0.002161	Intrusive rocks outcrops	0.026998
	Paleolandslides	0.000064	Conglomerates	0.002448
lowest classes	Elluvio-colluvial deposits	0.000056	Morainic sediments	0.001800
	Colonized scree slope	0.000010	Colonized scree slope	0.000086
Internal relief (m ha^{-1})	105.4 - 349.2	0.001095	105.4 - 349.2	0.039923
highest classes	91.7 - 105.4	0.000684	91.7 - 105.4	0.024036
	82.2 - 91.7	0.000473	82.2 - 91.7	0.014005
	37.0 - 49.3	0.000116	37.0 - 49.3	0.002160
lowest classes	19.2 - 37.0	0.000090	19.2 - 37.0	0.000549
	0 - 19.2	0.000029	0 - 19.2	0.000080
Planar curvature (100 m^{-1})	-21.51 - -1.26	0.001257	-21.51 - -1.26	0.038161
highest classes	1.66 - 22.25	0.000453	1.66 - 22.25	0.013184
	-1.26 - -0.57	0.000408	-1.26 - -0.57	0.012720
	0.29 - 0.63	0.000172	0.29 - 0.63	0.004851
lowest classes	-0.23 - -0.06	0.000151	0.11 - 0.29	0.004564
	-0.06 - 0.11	0.000108	-0.06 - 0.11	0.003392

Factor map	GeoIFFI		GeoIFFI-N		GeoIFFI-C		GeoIFFI-S		DF2001		DF2001-N		DF2001-C		DF2001-S	
	A	***R***	***A***	***R***	***A***	***R***	***A***	***R***	***A***	***R***	***A***	***R***	***A***	***R***	***A***	***R***
Altitude	**83.68**	0.07	**92.16**	0.03	79.73	0.01	82.78	0.03	88.07	2.17	82.17	**1.36**	**94.01**	0.43	**95.48**	0.83
Aspect	39.95	0.04	60.48	0.02	73.42	0.01	75.15	0.02	61.13	1.21	64.59	0.43	55.20	0.33	83.79	0.57
Fault distance	35.95	0.05	53.49	0.02	65.32	0.01	75.75	0.02	42.06	1.73	47.68	0.41	70.31	0.34	81.05	0.74
Internal relief	63.1	0.07	72.74	0.02	84.68	0.01	67.22	0.04	73.41	**2.57**	78.54	0.90	87.83	0.52	68.50	**1.06**
Land use	76.85	**0.08**	88.59	0.04	65.77	0.01	82.78	0.03	**91.91**	2.31	**95.98**	0.93	78.63	**0.69**	89.43	0.99
Geology	77.12	**0.08**	80.41	**0.04**	81.08	0.01	**83.68**	0.04	84.72	2.31	91.72	1.35	80.82	0.52	86.10	1.03
Slope	67.3	**0.08**	66.61	0.03	65.77	0.01	59.28	**0.0470**	70.77	2.38	86.13	0.70	85.58	0.49	64.91	0.96
Planar curvature	58.84	0.07	64.05	0.03	56.31	**0.01**	62.28	0.0260	60.26	2.11	62.86	0.72	65.09	0.53	55.82	0.87
Profile curvature	35.68	0.05	65.59	0.02	55.86	0.01	41.02	0.03	43.21	1.3	54.43	0.39	48.56	0.29	44.28	0.59
Flow accumulation	83.06	0.03	81.95	0.01	**86.14**	0.01	83.02	0.0153	88.87	1.03	87.09	0.33	90.48	0.24	89.34	0.46

Inventory	SRC	PRC	Factor maps
GeoIFFI	85.74	84.15	altitude, land use, geology, slope, profile curvature, planar curvature, flow accumulation
DF2001	87.16	88.37	altitude, land use, geology, slope, planar curvature, flow accumulation

Inventory	SRC	Factor maps
GeoIFFI-N	87.88	altitude, landuse, geology, slope, internal relief, planar curvature
GeoIFFI-C	84.48	altitude, aspect, faults, landuse, geology, slope, internal relief, planar curvature
GeoIFFI-S	89.51	altitude, aspect, faults, landuse, geology, slope, internal relief, planar curvature, flow accumulation
DF2001-N	92.88	altitude, aspect, landuse, geology, slope, internal relief, planar curvature
DF2001-C	91.75	altitude, aspect, faults, landuse, geology, slope, internal relief, planar curvature
DF2001-S	90.96	altitude, aspect, faults, landuse, geology, slope, internal relief, planar curvature

Inventory	PRC	Factor maps
GeoIFFI-N	76.42	altitude, landuse, geology, slope, internal relief, planar curvature
GeoIFFI-C	80.28	altitude, aspect, faults, landuse, geology, slope, internal relief, planar curvature
GeoIFFI-S	77.78	altitude, aspect, faults, landuse, geology, slope, internal relief, planar curvature, flow accumulation
DF2001-N	82.33	altitude, aspect, landuse, geology, slope, internal relief, planar curvature
DF2001-C	87.39	altitude, aspect, faults, landuse, geology, slope, internal relief, planar curvature
DF2001-S	88.35	altitude, aspect, faults, landuse, geology, slope, internal relief, planar curvature

GeoIFFI-S	75.09		
DF2001-R	81.11	73.53	
DF2001-S	70.80	75.55	71.95
	GeoIFFI-R	GeoIFFI-S	DF2001-R

	VH	H	M	L	Total
GeoIFFI Random					
% of landslides	55.38	26.88	13.61	4.13	100.00
Landslide density	0.00181	0.00044	0.00022	0.00003	0.00033
GeoIFFI Spatial					
% of landslides	56.13	27.49	10.56	5.82	100.00
Landslide density	0.00184	0.00045	0.00017	0.00004	0.00033
DF2001 Random					
% of landslides	61.18	28.50	9.15	1.17	100.00
Landslide density	0.05941	0.01384	0.00444	0.00023	0.00971
DF2001 Spatial					
% of landslides	63.71	28.28	6.46	1.56	100.00
Landslide density	0.06186	0.01373	0.00314	0.00030	0.00971